



Research article



Effect of a Biodegradable Additive on the Mechanical Properties of LDPE Blown Films: A Statistical and Machine Learning Approach

Efecto de un aditivo biodegradable en las propiedades mecánicas de películas sopladas de LDPE: un enfoque estadístico y de aprendizaje automático

Gilberto Alarcón Aguilar¹ , Alam Josué Reyes López² , Frixia Galán-Méndez^{1*} 

¹Universidad Veracruzana, Facultad de Ciencias Químicas, Circuito Gonzalo Aguirre Beltrán s/n, zona Universitaria, Xalapa, Veracruz, México, C. P. 91000.

²Universidad Veracruzana, Maestría en Ingeniería de la Calidad, Circuito Gonzalo Aguirre Beltrán s/n, zona Universitaria, Xalapa, Veracruz, México, C. P. 91000.

Autor de correspondencia: Frixia Galán-Méndez, Universidad Veracruzana, Facultad de Ciencias Químicas, Circuito Gonzalo Aguirre Beltrán s/n, zona Universitaria, Xalapa, Veracruz, México, C. P. 91000. Correo electrónico: fgalan@uv.mx. ORCID:

Recibido: 5 de Julio del 2025

Aceptado: 19 de Junio del 2026

Publicado: 24 de Junio del 2026

Resumen. - El estudio evalúa el efecto que tiene la adición del compuesto biodegradable P-Life sobre las propiedades mecánicas de bolsas para hielo "IB", fabricadas a partir de polietileno de baja densidad (LDPE). Se recolectaron datos de resistencia a la tracción, elongación, resistencia al rasgado, resistencia al punzado e impacto durante un periodo de seis meses en una planta manufacturera. Se estudiaron correlaciones entre las propiedades mecánicas y las formulaciones con (B) y sin aditivo biodegradable (NB). El análisis de Pearson mostró correlaciones positivas entre el grosor de la película y sus propiedades ($r \geq 0.5$). El ANOVA reveló diferencias significativas ($p \leq 0.05$) entre ambas formulaciones en algunas propiedades. Además, se desarrolló un modelo predictivo mediante el algoritmo M5P con una precisión del 94.147%, validado con muestras reales. Los resultados sugieren que el uso de inteligencia artificial es viable para predecir propiedades mecánicas en procesos de extrusión de polímeros, lo que puede optimizar el control de calidad industrial.

Palabras clave: Extrusión soplada; Propiedades mecánicas; Polietileno; ANOVA; Aprendizaje automático.

Abstract.- This study evaluates the effect of incorporating the biodegradable additive P-Life on the mechanical properties of ice bags (IB) made from low-density polyethylene (LDPE). Mechanical resistance to tension, elongation, tearing, puncture, and impact was measured over a six-month production period. Correlations were analyzed between mechanical performance and the presence or absence of the additive. Pearson's coefficient indicated positive correlations ($r \geq 0.5$) between film thickness and mechanical properties. ANOVA revealed statistically significant differences ($p \leq 0.05$) in several properties depending on the formulation. In addition, a predictive model based on the M5P algorithm was developed, achieving 94.15% accuracy, and was validated with actual samples. The results suggest that machine learning is a viable tool for predicting mechanical behavior in polymer extrusion processes, offering improvements in industrial quality control.

Keywords: Blown film extrusion; Mechanical properties; Low-density polyethylene; ANOVA; Machine learning.



1. Introduction

In 2020, the food industry generated 826,000 tons of packaging, of which 239,000 tons were allocated to disposable products [1], [2]. Most of this packaging is manufactured with non-biodegradable plastics such as LDPE, resulting in considerable environmental impact [3], [4]. To address this problem, additives like P-Life—derived from coconut palm oil—have been developed to accelerate plastic degradation [5], [6].

Previous studies have demonstrated that these additives can modify the mechanical properties of plastic films depending on their molecular interactions [7], [8],[9]. Furthermore, the operating conditions of the extrusion process significantly influence these properties [10].

Despite advancements, modeling polymer transformation processes remains complex due to nonlinear relationships between variables [11], [12]. The use of machine learning tools, such as M5P algorithms, offers an alternative for predicting properties without resorting to costly experimental methods [13]–[16]. For instance, in the concrete industry, mechanical properties were predicted using the M5P artificial intelligence algorithm with approximately 97% accuracy [17].

Similarly, it has been employed in numerous materials science scenarios, facilitating the prediction of physical properties under temperature variations [18]. Additionally, this technology is also utilized to optimize processes where numerical data availability is not limited [19].

The M5P artificial intelligence algorithm excels particularly in predicting mechanical properties, unlike conventional regression methods [20]. Therefore, the objective of this work is to demonstrate the potential of the M5P algorithm for predicting the mechanical properties of LDPE films and to statistically evaluate the difference between formulations with and without biodegradable additives, providing evidence to support industrial implementation.

2. Materials and methods

2.1 Materials

Low-density polyethylene (LDPE) supplied by Braskem Indesa was used, characterized by its high mechanical strength and versatility for processes such as blown extrusion and injection molding (density: 0.932 g/cm³; melt flow index: 0.25 g/10 min at 190 °C/2.16 kg).

The biodegradable additive employed was P-Life, commercial name SMC 100, dosed at 1–3% by mass. This additive is designed for plastic films and exhibits a density of 1.2 g/cm³ and a melt flow index of 2–10 g/10 min.

2.2 Equipment used

An industrial TECOM extruder (OLGIATE OLONA, Italy) was employed, configured with a linear temperature profile of 185 °C in all zones, a mass flow rate of 45 kg/h, and a screw speed of 120 rpm.

For mechanical tests, a GBD-2 universal testing machine (Electronic Tensile Tester, China) was used, equipped with pneumatic grips at 6 bar pressure (Figure 1).



For impact testing, a GBD-12 universal testing machine (Falling Dart Impact Tester, China) was utilized, equipped with pneumatic holders at 6 bar pressure (Figure 2).



Figure 1. Universal testing machine GBD-2 *Electronic Tensile Tester*. (Source: Own elaboration).



Figure 2. Impact machine GBD-12 *Falling Dart Impact Tester*. (Source: Own elaboration).

2.3 Mechanical characterization

Samples were extracted from rolls intended for ice bag (IB) production, evaluated exclusively in the machine direction (MD) as established by the Mexican standard NMX-134-CNCP-2013. (Figure 3). Tests were conducted at room temperature ($23 \pm 2 \text{ }^{\circ}\text{C}$), in accordance with the corresponding Mexican standards.

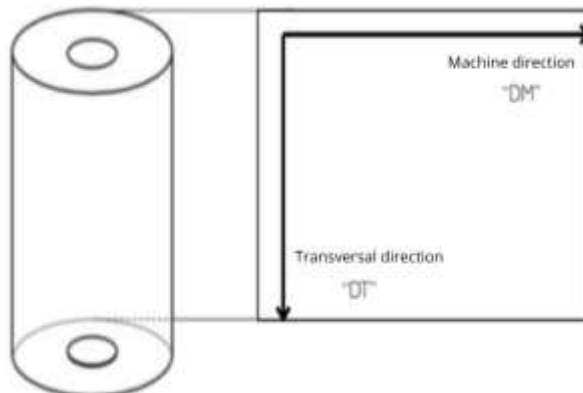


Figure 3. Extrusion direction of polyethylene film. (Source: own elaboration).



2.3.1 Tensile strength and elongation

Five test pieces were cut from the extruded film, their dimensions are 16 mm wide and 100 mm long, subsequently the testing machine was set to 100 mm/min with a separation between jaws of 50 mm (Figure 4), in accordance with the Mexican standard NMX-134-CNCP-2013.

2.3.2 Tearing and Puncture Resistance

Five specimens were cut per test. Tests were performed at 50 mm/min. For the tear, the grip separation was 25 mm (Figure 4), in accordance with Mexican standard NMX-E-112-CNCP-2014. In the puncture test, the needle made surface contact with the specimen, measuring 100 mm wide and 100 mm long.

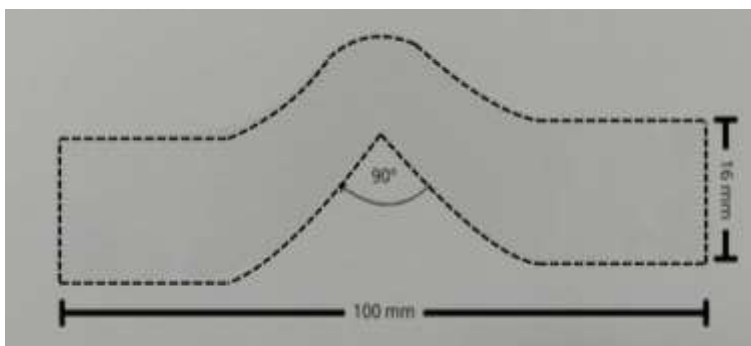


Figure 4. Specimen used in tearing resistance testing

2.3.3 Impact resistance

Eight test specimens were cut per test, each measuring 100 mm wide and 100 mm long. The dart was dropped from a height of 660 mm in free fall, impacting the specimen (Figure 7), in accordance with Mexican standard NMX-E-099-CNCP-2014.

2.4 Statistical analysis

Data was collected over six months, including operational conditions (extrusion, ambient, and coil temperatures), thickness, and mechanical properties (tensile strength, elongation, tearing, puncture, and impact resistance). The analysis consisted of two phases: 1) Exploration of correlations using Pearson's coefficient. 2) Analysis of variance (ANOVA) to evaluate the effect of formulation type, with thickness as a blocking factor. The assumptions of normality, homoscedasticity, and independence were validated through graphical residual analysis.

3 Results and discussion

Operating variables—particularly temperature and screw speed—significantly influence ($p \leq 0.05$) the mechanical properties of films produced by extrusion [7], [8]. In this context, Table 1 presents the key variables monitored during the blown extrusion process for manufacturing ice bags made from low-density polyethylene (LDPE).



Table 1. Variables in the blow molding extrusion process.

Variable	Lower limit	Upper limit	Range
Operating temperature (°C)	180	195	15
Operating pressure (bar)	350	350	N.A.
Upper roller pressure (bar)	3	4	1
Screw speed (rpm)	120	120	N.A.
Cooling (%)	40	60	20

Furthermore, Figure 8 shows the flow diagram of the blown extrusion process for polyethylene film formation. This diagram enables identification of the critical variables previously mentioned, which were considered for conducting the statistical analysis described in the following sections.

Table 2. Correlation of variables with the through the Pearson method.

Variables	Caliber (ga)	Calibration (%)	T. coil (°C)	T. extruder (°C)	Ambient temperature (°C)	Tensile strength (Mpa)	Elongation (%)	R. torn (kgF)	R. punching (N)
Calibration (%)	-0.042								
T. Coil (°C)	-0.134	0.067							
T. extruder (°C)	-0.081	0.277	-	0.302					
Ambient temperature (°C)	-0.150	-0.028	0.768	-0.119					
Tensile strength (Mpa)	0.869	-0.066	-	0.006	-0.237				
Elongation (%)	0.685	-0.152	-	-0.181	-0.111	0.692			
R. torn (kgF)	0.860	-0.015	-	0.109	-0.180	0.778	0.498		
R. punching (N)	0.786	-0.019	-	0.139	-0.375	0.764	0.489	0.708	
Impact (g)	0.533	0.083	-	0.034	-0.257	0.527	0.543	0.407	0.533

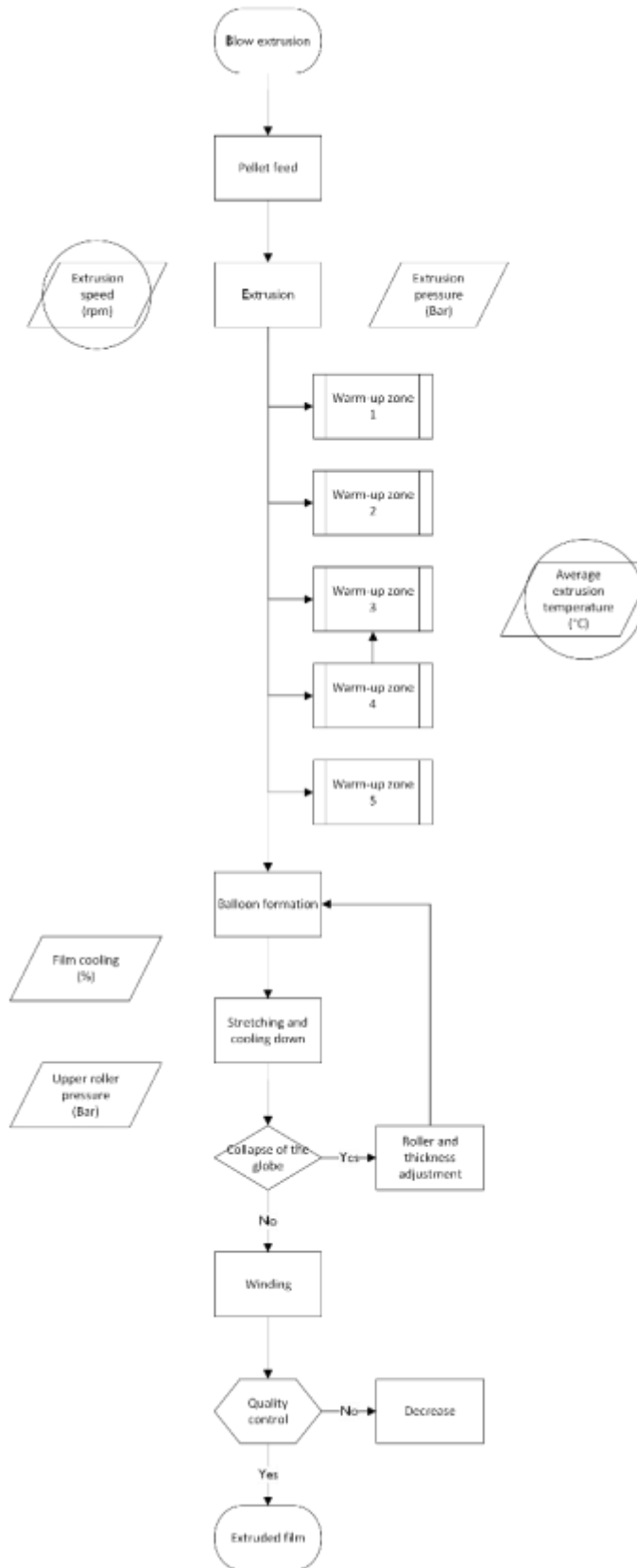


Figure 5. Flow diagram of the blown extrusion.

Based on 40 observations—which included the independent variables of actual thickness, thickness deviation, and average temperatures of the coil, extruder, and ambient, along with the mechanical properties of tensile strength, elongation, tearing resistance, puncture resistance, and impact resistance—the Pearson correlation coefficient was calculated using Minitab 2021, as shown in Table 2. We selected Pearson's correlation coefficient to demonstrate potential relationships between variables, as reported by Temizhan et al. [21], since this methodology is highly efficient for revealing correlations in real-world data.

The results show ($r \geq 0.5$) a positive and significant correlation between actual thickness, and all evaluated mechanical properties (tensile strength, elongation, tearing resistance, puncture resistance, and impact resistance). Likewise, a significant association was detected between ambient temperature and coil temperature—a phenomenon consistent with the second law of thermodynamics: heat flows from the higher-temperature system (coil) toward the lower-temperature system (ambient) until equilibrium is reached, driven by the existing thermal gradient. Tensile strength, in turn, exhibited positive correlations with the remaining mechanical properties. The direct relationship with elongation is particularly notable: the higher the maximum force sustained before rupture, the greater the unit deformation recorded by the film reflecting a more ductile polymer matrix. Analogous reasoning extends to tearing, puncture, and impact tests, which share the principle of subjecting the film to separation stresses until failure. Finally, elongation showed a positive correlation with impact resistance. During free-fall impact testing, the film undergoes extensive deformation; consequently, high elongation performance translates predictably into greater energy absorption capacity before fracture.



These findings confirm that the analyzed mechanical properties are strongly interrelated and underscore the importance of controlling thickness and thermal process variables to ensure consistent mechanical performance in extruded LDPE films.

3.1 Analysis of variance with thickness as a blocking factor

To identify statistically significant differences in mechanical properties based on formulation, an analysis of variance (ANOVA) was performed using a set of 50 observations. Thickness was incorporated as a blocking factor to control its influence on system variability. Box-Cox transformations were applied to the response variables to better satisfy ANOVA's assumptions of normality and homogeneity of variances by Atkinson, *et al.* [22].

The analysis began by evaluating the effect of "thickness" and "formulation" factors on tensile strength, employing a Box-Cox transformation with parameter $\lambda = 2$. Subsequently, variance analysis was conducted using the transformed variable as the response.

Table 3 shows the ANOVA results, demonstrating that thickness has a significant effect on the film's tensile strength ($p \leq 0.05$), while no statistically significant differences attributable to the formulation were observed.

Table 3. Analysis of variance for response tensile strength transform.

Source	GL	SC Adjustment	MC Adjustment	F value	P-value
Biodegradable	1	16749	16749	0.19	0.667
Caliber	7	60620038	8660005	96.08	0.000
Error	241	21721776	90132		
Total	249	82355274			

The residual analysis indicated that the statistical assumptions required for model validity were met as residuals are normally distributed, centered around zero, exhibit no heteroscedasticity patterns, and show no autocorrelation. Consequently, the assumptions of normality, homoscedasticity, and independence were verified. Additionally, a post hoc multiple comparison test using Fisher's method (LSD) was applied to explore in greater detail the differences between the levels of the identified significant factor, as demonstrated by Lu *et al.*, [23], these results are shown in Table 4.

Table 4. Fisher's LDS method and a 95% confidence (tensile strength).

Caliber (ga)	N	Average (MPa)	Group
300	15	54.009	A
220	15	37.770	B
190	5	37.445	B
200	20	35.242	B C
210	20	32.613	C D
175	65	30.449	D E
180	10	29.644	E



170	10	26.022	F
-----	----	--------	---

The results show an upward trend in tensile strength as thickness increases. The lowest strength was recorded in thin films, with highly significant differences between the 170 ga thickness (26.0 MPa) and the 300 ga thickness (54.0 MPa). This behavior aligns with the Pearson correlation analysis, which showed a direct association between thickness and mechanical properties.

When comparing these values with those reported by Mallegni *et al.* [24]—who analyzed a plasticized PLA/PBAT film of 0.05 mm (\approx 200 ga) with a strength of 25 MPa—it is observed that a film of identical thickness manufactured primarily from low-density polyethylene achieves a substantially higher mean strength (35.2 MPa). This difference can be attributed to both material composition and process conditions: in the present study the extruder operated at 120 rpm, whereas Mallegni *et al.* [24] employed 200 rpm; this influence of screw speed on mechanical properties was previously documented by Gálvez *et al.* [8].

To analyze the effect of thickness and formulation on elongation, a Box-Cox transformation with $\lambda = 3$ was applied before conducting the ANOVA, ensuring compliance with normality and homogeneity of variances assumptions.

Table 5 presents the ANOVA results for the elongation variable, showing that thickness constitutes a statistically significant factor ($p \leq 0.05$), while no significant effects attributable to the formulation were detected. Residual analysis confirmed model assumption compliance: errors are normally distributed, centered around zero, with no relevant violations of homoscedasticity or evidence of autocorrelation, validating residual independence.

Table 5. Analysis of variance for response elongation transform.

Source	GL	SC Adjustment	MC Adjustment	F value	P-value
Biodegradable	1	165	165	0.04	0.841
Caliber	7	1173067	167581	40.82	0.000
Error	241	959391	4105		
Total	249	2168610			

Subsequently, Fisher's post hoc test (LSD) was applied to perform multiple comparisons between the levels of the significant factor, the results of which are presented in Table 6.

Table 6. Fisher's LDS method and a 95% confidence (elongation).

Caliber (ga)	N	Average (%)	Group
300	15	832.725	A
190	5	737.113	B
210	20	691.023	B C
200	20	688.613	B C
220	15	678.024	C



180	100	633.386	D
175	65	612.068	D
170	10	611.669	D

The data reveals a direct relationship between film thickness and elongation: greater thickness yields higher elongation resistance. The thinnest films showed the lowest elongation values, with a statistically significant difference between the 170 ga thickness (611.67%) and 300 ga thickness (832.73%). This behavior is primarily attributed to increased film thickness, which enhances material stretching during extrusion—consistent with the Pearson correlation analysis showing a positive association between thickness and elongation.

These results can be compared to those reported by Aliotta *et al.* [25], who documented elongation percentages of 48.77%, 107.94%, and 295.8% for specimens averaging 160 ga thickness. Contrasted with this study’s average for 170 ga films (the thinnest set) of 611.67%, a notable difference emerges. Although formulations differ, the results indicate that low-density polyethylene (LDPE) films exhibit higher ductility than those composed of polylactic acid (PLA) and polybutylene succinate adipate (PBSA).

Another relevant factor is extruder screw speed. The comparative study operated at 300 rpm—significantly higher than the 120-rpm used here. According to Gálvez *et al.* [8], increased rpm can adversely affect mechanical properties, suggesting observed differences may also be influenced by this operating parameter.

Complementarily, Mallegni *et al.* [24] reported average elongation near 250% for a 200 ga film composed primarily of PLA/PBAT with a plasticizer (Ej400). In this study, the same thickness (200 ga) achieved an average elongation of 688.61%, reinforcing LDPE’s superior deformability. The plasticizer in comparative study likely impaired mechanical properties, reducing elongation capacity.

Additionally, Gómez-Bachar *et al.* [26], reported elongation in the range of 170–530% for films composed primarily of starch with an approximate thickness of 250 ga, demonstrating that biodegradable compounds can be equally resistant as non-biodegradable ones according to Itabatana *et al.* [11].

Also, Kim *et al.* [27], reported that the addition of biodegradable compound based on rice husks in 0.5% composition is as resistant as the extruded film from LDPE, [11].

Furthermore, the effect of "thickness" and "formulation" factors on tearing resistance was analyzed. A Box-Cox transformation with parameter $\lambda = 0.5$ was applied before conducting the corresponding ANOVA.

Table 7 presents the ANOVA results for film tearing resistance. The data confirms that thickness is a statistically significant factor ($p \leq 0.05$) for this mechanical property, while no significant differences attributable to formulation were identified.

Table 7. Analysis of variance for response tear strength transformation.

Source	GL	SC Adjustment	MC Adjustment	F value	P-value
--------	----	---------------	---------------	---------	---------



Biodegradable	1	0.00233	0.002325	1.19	0.275
Caliber	7	0.80578	0.115112	59.14	0.000
Error	241	0.46908	0.001946		
Total	249	1.2749			

Residual analysis confirmed compliance with the statistical model assumptions: errors are normally distributed, exhibit no heteroscedasticity, and are independent, thereby validating the ANOVA model application. Based on these results, a multiple comparisons test was performed using Fisher's method (LSD), the results of which are presented in Table 8.

Table 8. Fisher's LDS method and a 95% confidence (tear strength).

Caliber (ga)	N	Average (kgF)	Group
300	15	0.871318	A
220	15	0.729295	B
210	20	0.617177	C
200	20	0.605968	C D
190	5	0.541330	D E
170	10	0.532694	E
180	100	0.531749	E
175	65	0.518209	E

The results show a direct relationship between film thickness and tearing resistance: greater thickness requires higher force to induce tearing fracture. The thinnest films exhibited the lowest resistance values, with a statistically significant difference between the 170 ga thickness (0.532 kgf) and 300 ga thickness (0.871 kgf).

This behavior is primarily attributed to extruded film thickness, which directly influences structural integrity. As evidenced by Pearson correlation analysis, a positive linear relationship exists between thickness and tearing resistance. Consequently, increased material thickness systematically enhances its capacity to withstand shear stresses—consistent with expected behavior for extrusion-processed polymer films.

These results can be compared to Aliotta *et al.* [25] and Mallegni *et al.* [24], who documented tearing resistances of 5.24 N/mm for 200 ga films and 4.69 N/mm for 160 ga films, respectively. Although formulations differ, thick variations likely explain observed differences. For comparison, the force per millimeter was calculated from reported values, yielding 0.0267 kgf and 0.0189 kgf, respectively. These contrast with this study's results for 170 ga and 200 ga thicknesses (0.5326 kgf and 0.6059 kgf), confirming polyethylene films exhibit superior tearing resistance compared to primarily polylactic acid (PLA)-based films [28], [29].

This significant difference can be attributed to multiple factors: extrusion speed, formulation, and experimental conditions. Crucially, this study's tests followed the Mexican standard NMX-E-112-CNCP-



2014—applicable in the company's jurisdiction—hence results may differ from those obtained under region-specific regulations.

This contrast is supported by Zhu et al. [30], who point out that PLA and PBAT offer favorable degradability and high transparency, making them attractive for industrial applications. However, their low mechanical strength necessitates recent efforts to improve the composite properties for packaging applications.

Subsequently, the effect of "thickness" and "formulation" factors on puncture resistance was re-evaluated. The optimal Box-Cox transformation parameter was $\lambda = 1$, so no transformation was applied to the response variable.

Table 9 presents the ANOVA results for film puncture resistance. The data confirms that both thickness and formulation are statistically significant factors ($p \leq 0.05$) affecting this mechanical property, the only property where both factors demonstrated relevant effects.

Table 9. Analysis of variance for punching resistance.

Source	GL	SC Adjustment	MC Adjustment	F value	P-value
Biodegradable	1	0.5166	0.51663	9.75	0.002
Caliber	7	20.1195	2.87421	54.26	0.000
Error	241	12.7665	0.05297		
Total	249	33.2135			

Residual analysis confirmed compliance with ANOVA assumptions, including normality, homoscedasticity, and error independence. Consequently, a post hoc multiple comparisons test was performed using Fisher's method (LSD), the results of which are presented in Table 10.

Table 10. Fisher's LDS method and 95% confidence (punching strength).

Caliber (ga)	N	Media (N)	Group
300	15	3.26423	A
220	15	2.64553	B
210	20	2.38496	C
200	20	2.35424	C
190	5	2.31459	C D
170	10	2.16301	D
180	100	2.15539	D
175	65	1.98779	E

The results show a direct relationship between film thickness and puncture resistance: greater thickness requires higher force to fracture the material. The thinnest films exhibited the lowest resistance, with a statistically significant difference between 170 ga (2.16 N) and 300 ga (3.26 N) thickness. This behavior



is primarily attributed to extruded film thickness, confirming the positive association observed in the Pearson correlation analysis.

Furthermore, according to the means presented in Table 11, the biodegradable formulation demonstrated superior puncture resistance compared to the non-biodegradable formulation, suggesting enhanced mechanical performance of additive-containing materials under the evaluated conditions.

Table 11. Average punching resistance by formulation.

Biodegradable	Punching resistance (N)	Deviation standard
Yes	2.29	0.32
No	2.25	0.28

Furthermore, the effect of thickness and formulation factors on impact resistance was evaluated. To satisfy ANOVA assumptions, a Box-Cox transformation with parameter $\lambda = -1$ was applied to the response variable. Subsequently, variance analysis was conducted using the transformed variable.

Table 12 presents the ANOVA results, demonstrating that both thickness and formulation are statistically significant factors ($p \leq 0.05$) for the film's impact resistance. Residual analysis confirmed compliance with ANOVA assumptions, including normality, homoscedasticity, and independence. Consequently, a post hoc multiple comparisons test was performed using Fisher's method (LSD), the results of which are shown in Table 13.

Table 12. Analysis of variance for response impact resistance transformation.

Source	GL	SC Adjustment	MC Adjustment	F value	P-value
Biodegradable	1	0.000002	0.000002	5.80	0.017
Caliber	7	0.000071	0.000010	38.51	0.000
Error	241	0.000064	0.0000000		
Total	249	0.000136			

Table 13. Fisher's LSD method and a 95% confidence (impact resistance).

Caliber (ga)	N	Media (g)	Group
300	15	456.635	A
220	20	281.081	B
210	15	271.896	B C
175	65	248.846	D
200	20	241.416	D E
190	5	239.725	C D E F
180	100	229.813	E F
170	10	216.818	F

The data demonstrates a positive relationship between film thickness and impact resistance: greater thickness requires higher force to puncture the material. Thinner films recorded the lowest impact



resistance values, with a statistically significant difference between 170 ga (216.82 g) and 300 ga (3456.64 g) thicknesses.

This behavior is primarily attributed to extruded film thickness, confirmed by correlation analysis showing a positive association between these variables. Therefore, increased thickness systematically enhances the material's impact resistance capacity.

Additionally, according to the means reported in Table 14, the biodegradable formulation showed lower impact resistance compared to the non-biodegradable formulation, suggesting a trade-off between biodegradability and performance for this mechanical property.

Table 14. Average impact resistance by formulation.

Biodegradable	Impact resistance (g)	Deviation standard
Yes	259.68	56.65
No	268.10	48.07

When contrasting this study's results with those reported by Chai [10]—who documented average impact resistance values of 456.64 g for 300 ga films and 775 g for 100 ga films—it is observed that the film thickness analyzed here is approximately three times greater, correlating with superior resistance in free-fall impact testing.

This difference can be attributed to varying experimental conditions and material types. In this study, processing speed was 120 rpm, and the extrusion temperature range was maintained between 180 and 195 °C. As evidenced by Gálvez *et al.* [8], processing speed is a critical factor for extruded films' mechanical properties.

Furthermore, experimental conditions—including applicable standards—directly influence results. This study employed the Mexican standard NMX-E-099-CNCP-2014, which specifies a free-fall drop height of 660 mm for the test dart. Variations in this height modify the applied potential energy upon impact, affecting measured resistance.

Additionally, material types decisively affect mechanical properties. Films with biodegradable additives exhibited lower impact and puncture resistance compared to non-biodegradable formulations, suggesting a trade-off between biodegradability and material robustness.

3.2 Property regression models mechanics based in decision trees.

To describe and predict the mechanical properties of films based on variables such as thickness, thickness deviation, extrusion temperature, and formulation, the M5P algorithm was applied. This method constructs decision trees using the *weighted reduction of standard deviation* as the node-splitting criterion, fitting



linear regression models at terminal leaves. This constructs a decision tree where the splits are determined by the weighted reduction in the standard deviation of the target variable. A linear regression is fitted to each terminal leaf, allowing the tree segmentation to be combined with the precision of linear models. The weighting expression for node splitting is shown in [31]:

$$SDR = \frac{M}{|T|} * \beta(i) * \left[sd(T) - \sum_{j \in \{L,R\}} \frac{|T_j|}{|T|} * sd(T_j) \right] \tag{1}$$

As to:

$\frac{M}{|T|}$ = Proportion of examples without missing values for the evaluated attribute.

$\beta(i)$ = Correction factor that penalizes attributes with many values.

$sd(T)$ = Standard deviation of the class values at the current node T.

$\sum_{j \in \{L,R\}} \frac{|T_j|}{|T|}$ = Weighed sum of the standard deviations of the left (L) and right (R) sub nodes.

To apply the M5P algorithm for modeling the mechanical properties of films based on operating variables, WEKA software version 3.9.6 was used. To obtain models with optimal fit, various transformations were evaluated for the response variables, selecting those exhibiting the highest correlation coefficient. The identified optimal transformations are presented in Table 15.

Table 15. Transformations with best fit from the correlation coefficient.

Property mechanics	Transformation
Tensile strength	Quadratic
Elongation	Logarithmic
Tear resistance	Quadratic
Punching resistance	Quadratic

Furthermore, since the primary hyperparameter of the M5P algorithm corresponds to the minimum number of instances required to fit the model at each leaf, different criteria were evaluated by varying this parameter. Specifically, varying minimum instance quantities per leaf were analyzed for linear model estimation. Table 16 presents the correlation coefficients obtained for each mechanical property across different minimum instance per leaf values.

Table 16. Correlation coefficients varying the minimums instances per sheet (R).

Instances per sheet	Tensile strength	Elongation	Tear resistance	Punching resistance
2	0.6557	0.4662	0.8047	0.5746
4	0.6557	0.4662	0.8047	0.5746
6	0.6533	0.4999	0.7825	0.5811
8	0.6547	0.4943	0.7827	0.5811
10	0.6713	0.5266	0.7925	0.5811



12	0.6680	0.4784	0.7929	0.5811
14	0.6652	0.4849	0.7817	0.5771

As observed, the mechanical property best described by the input data (thickness, thickness deviation, extrusion temperature, and formulation) is tearing resistance, with a correlation coefficient of 0.8047 obtained when training a model using 4 minimum instances per leaf. Conversely, tensile strength exhibited a correlation coefficient of 0.6713 with 10 minimum instances per leaf. It is worth mentioning that the mathematical models presented below are expressed according to their respective linearization used to apply the algorithm.

This result can be compared to that reported by [32], where a decision tree algorithm applied to experimental tensile strength data for high-density polyethylene (HDPE) films achieved a correlation coefficient of 0.94 and a mean absolute error of 0.04 with 14 minimum instances per leaf. The lower correlation in this study may be explained by different predictor variables: while [32] used only operating temperatures and mechanical properties, the present work also considered material-specific variables like density and melt flow index—whose inclusion could improve model fit as noted in [14] .

For elongation and puncture resistance, correlation coefficients of 0.5266 and 0.5811 were obtained, respectively. These values indicate that while the models partially explain the variation in these properties, other unconsidered variables affect their behavior, and their inclusion could enhance predictive capability.

The tearing resistance model is presented in Equation (2). Its utility lies in evaluating whether a process—under established conditions and with specific thickness—meets customer specifications. This property is particularly relevant given the high correlation (0.8047) achieved in the final model.

$$\text{Tearing } r. = 0.000011 * Cr + 0.000008 * Te - 0.307354 \quad (2)$$

As to:

Cr = Actual caliber of the film.

Te = Extrusion temperature.

The model obtained for tearing resistance consists of a single rule, indicating a linear fit between this property and the average extrusion temperature. The mean absolute error was 0.0482, equivalent to 0.2195 kgf, considering the tearing resistance data underwent quadratic transformation.

For tensile strength, a quadratic transformation was similarly applied, and the optimal model is shown in Equations (3) and (4), using actual thickness as the splitting criterion.

$$Cr \leq 31289.4165$$

$$\text{Tensile } r. = 0.011109 * Cr + 515.45731 \quad (3)$$

$$Cr > 31289.4165$$



$$\text{Tensile } r. = 101.227387 * B + 0.014527 * Cr + 556.00864 \quad (4)$$

As to:

B = Biodegradable (No=0, Yes=1).

Cr = Actual caliber of the film.

As observed, the obtained model consists of two rules, where the actual thickness selects one of the two presented linear models. For thicknesses greater than 31,289.4165 ga, formulation becomes particularly relevant, as the second linear model includes a term corresponding to formulation—assigned a value of 1 for non-biodegradable formulations and 0 for biodegradable formulations.

This behavior is explained by the P–Life biodegradable additive, incorporated at 1% mass proportion. Its primary function is to break long-chain polyethylene polymers into shorter molecules (oligomers) through an oxidation process typically activated by ultraviolet light, heat, and oxygen.

Regarding model performance, the mean absolute error was 154.4205 (transformed), equivalent to 12.4266 MPa, considering a quadratically transformed model. The models for elongation and puncture resistance are presented in Equations (5) and (6).

$$\text{Elongation} = 0.475258 * Cr - 0.121955 * D + 4.331964 \quad (5)$$

As to:

Cr = Actual caliber of the film.

D = Film miscaliber.

$$\text{Punching } r. = 0.000094 * Cr + 0.00008 * Te - 0.984355 \quad (6)$$

As to:

Cr = Actual caliber of the film.

Te = Extrusion temperature.

The correlation coefficients for elongation and puncture resistance were 0.5266 and 0.5811, respectively. Similarly, the mean absolute error (MAE) was 0.0666 for elongation and 0.7389 for puncture resistance, equivalent to a percentage error of 1.069% for elongation and an absolute error of 0.860 N for puncture resistance.

For these two mechanical properties, it is necessary to include additional variables to increase the explained variance percentage, improve the correlation coefficient, and reduce model prediction errors. Notably, logarithmic transformations were applied for elongation and quadratic transformations for puncture resistance.



The decision tree-based regression model was evaluated with 10 independent samples excluded from the training set. The test results, including the error associated with each mechanical property, are presented in Table 17.

Table 17. Testing the decision tree model.

Proof	Error in tensile strength	Error in elongation	Error in tear resistance	Error in punching resistance
1	1.210	5.178	2.070	3.607
2	1.795	2.622	0.695	2.902
3	3.788	12.602	0.196	6.076
4	4.277	13.877	3.701	0.583
5	6.903	10.626	0.543	9.303
6	0.108	13.766	4.444	11.259
7	3.184	0.035	2.959	3.163
8	22.101	6.289	9.411	1.291
9	9.446	6.849	13.211	14.135
10	1.878	1.956	9.817	6.250

Based on the data from Table 17, the average error for each mechanical property was calculated to quantify individual errors. The resulting values are presented in Table 18.

Table 18. Average error for each property mechanics.

Error in tensile strength (%)	Error in elongation (%)	Error in tear resistance (%)	Error in punching strength (%)
5.469	7.380	4.705	5.857

Finally, based on the data presented in Table 18, the overall average error was calculated, yielding a value of 5.853%. This quantifies the decision tree-based regression model's accuracy for predicting mechanical properties at 94.147%. This accuracy level is validated according to the ASME V&V 20-2021 standard—primarily used to quantify model accuracy against experimental data—which deems a model acceptable when achieving overall accuracy $\geq 90\%$ [33, 34].

These results demonstrate the efficacy of machine learning algorithms for modeling mechanical properties in polymer manufacturing processes. Specifically, nonlinear decision tree-based methods are essential for capturing complex multivariable relationships and optimizing production. Moreover, the ability to identify key data patterns—such as formulation and processing parameters—reinforces these models' industrial utility by reducing reliance on empirical testing and enhancing quality control.

4 Conclusion

This study evaluated the impact of the biodegradable additive P-Life on the mechanical properties of low-density polyethylene (LDPE) films for ice bags and developed a predictive model based on artificial intelligence. The ANOVA results identified film thickness as the most influential factor for tensile strength, elongation, and tear resistance, showing statistically significant differences ($p \leq 0.05$). In contrast, the formulation (with or without the biodegradable additive) did not exhibit a significant effect on these same properties. However, a discernible influence of P-Life was observed on puncture and impact resistance. This selective effect can be attributed to the



additive's mechanism of action, which is designed to initiate degradation through an oxidation process. By acting as localized sites for stress concentration, these modifiers alter the material's ability to absorb energy under point loads or impact, thereby modifying these specific properties without significantly affecting the behavior under tensile or tearing stresses.

The M5P machine learning algorithm proved to be an effective tool, predicting mechanical properties with an accuracy of 94.147%. This validates its utility for optimizing the extrusion process and reducing reliance on empirical testing methods. Collectively, this work confirms that while thickness is the critical parameter for most mechanical properties, the incorporation of the P-Life additive introduces specific changes in the material's performance. Furthermore, it corroborates the feasibility of implementing artificial intelligence models for quality control and the development of more sustainable flexible packaging.

5. Authorship acknowledgements

Gilberto Alarcón Aguilar: Conceptualization; Ideas; Methodology; Research; Writing; Original Draft. *Alam Josué Reyes López*: Conceptualization; Data Analysis. *Frixia Galán-Méndez*: Conceptualization; Methodology; Formal Analysis; Research; Writing; Revision and Editing; Project Management.

References

- [1] I. Santos Silva et al., "Malt bagasse in extruded wheat flour and PBAT biodegradable films," *Ind. Crops Prod.*, vol. 220, p. 119274, Nov. 2024, doi: 10.1016/j.indcrop.2024.119274.
- [2] A. Martínez-Camacho et al., "Extruded films of blended chitosan, low density polyethylene and ethylene acrylic acid," *Carbohydr. Polym.*, vol. 91, pp. 666–674, Aug. 2012, doi: 10.1016/j.carbpol.2012.08.076.
- [3] H. Najahi et al., "Plastic pollution in food packaging systems: Impact on human health, socioeconomic considerations and regulatory framework," *Elsevier B.V.*, May 2025, doi: 10.1016/j.hazadv.2025.100667.
- [4] B. Ucpinar, F. Ugur, and A. Aytac, "Active packaging films based on poly(butylene succinate) films reinforced with alkaline halloysite nanotubes: Production, properties, and fruit packaging applications," *Appl. Clay Sci.*, vol. 256, p. 107517, Jul. 2024, doi: 10.1016/j.clay.2024.107517.
- [5] L. Yi et al., "Simple but efficient preparation of high-strength, heat-resistant, and high-barrier PLA/TOBC plastic packaging containers via Pickering emulsion," *Compos. Commun.*, vol. 56, p. 102420, Jun. 2025, doi: 10.1016/j.coco.2025.102420.
- [6] P-Life American, "Aditivos plásticos biodegradables. Plásticos biodegradables, una realidad," *plifeamerican.com*. <https://plifeamerican.com> (accessed May 5, 2025).
- [7] T. Zhang, W. Han, C. Zhang, and Y. Weng, "Effect of chain extender and light stabilizer on the weathering resistance of PBAT/PLA blend films prepared by extrusion blowing," *Polym. Degrad. Stabil.*, vol. 183, p. 109455, Jan. 2021, doi: 10.1016/j.polymdegradstab.2020.109455.
- [8] J. Gálvez et al., "Effect of extrusion screw speed and plasticizer proportions on the rheological, thermal, mechanical, morphological and superficial properties of PLA," *Polymers*, vol. 12, no. 9, p. 2111, Sep. 2020, doi: 10.3390/polym12092111.



- [9] H. Wu et al., "Mechanical activation-enhanced metal-organic coordination strategy to Fabricate high-performance starch/polyvinyl alcohol films by extrusion blowing," *Carbohydr. Polym.*, vol. 333, p. 121982, Feb. 2024, doi: 10.1016/j.carbpol.2024.121982.
- [10] C. K. Chai, "Rheological studies of molecular effect and processing conditions on blown film property of polyethylenes," *Polymer*, vol. 267, p. 125668, Feb. 2023, doi: 10.1016/j.polymer.2022.125668.
- [11] B. E. Itabana, A. K. Pal, A. K. Mohanty, and M. Misra, "Biodegradable blown film composite from poly(butylene adipate-co-terephthalate) and talc: Effect of uniaxial stretching on mechanical and barrier properties," *Food Packag. Shelf Life*, vol. 39, p. 101147, Nov. 2023, doi: 10.1016/j.fpsl.2023.101147.
- [12] J. Park, K.-Y. Kim, and R. Sohmshetty, "A prediction modeling framework: Toward integration of noisy manufacturing data and product design," *ASME*, 2015. [Online]. Available: <http://www.asme.org/about-asme/terms-of-use>
- [13] H. A. Dahish and A. D. Almutairi, "Compressive strength prediction models for concrete containing nano materials and exposed to elevated temperatures," *Results Eng.*, vol. 25, p. 103975, Mar. 2025, doi: 10.1016/j.rineng.2025.103975.
- [14] S. Altarazi, R. Allaf, and F. Alhindawi, "Machine learning models for predicting and classifying the tensile strength of polymeric films fabricated via different production processes," *Materials*, vol. 12, no. 9, p. 1475, 2019, doi: 10.3390/ma12091475.
- [15] S. K. Dang and Singh, "Predicting tensile-shear strength of nugget using M5P model tree and random forest: An analysis," *Comput. Ind.*, vol. 124, p. 103345, Jan. 2021, doi: 10.1016/j.compind.2020.103345.
- [16] C. Herriott and A. D. Spear, "Predicting microstructure-dependent mechanical properties in additively manufactured metals with machine- and deep-learning methods," *Comput. Mater. Sci.*, vol. 175, p. 109599, Apr. 2020, doi: 10.1016/j.commatsci.2020.109599.
- [17] M. Abdallah et al., "The Machine-Learning-Based Prediction of the Punching Shear Capacity of Reinforced Concrete Flat Slabs: An Advanced M5P Model Tree Approach," *Appl. Sci.*, vol. 13, p. 8325, Jul. 2023, doi: 10.3390/app13148325.
- [18] C. Machello et al., "Tree-based machine learning approach to modelling tensile strength retention of Fibre Reinforced Polymer composites exposed to elevated temperatures," *Compos. Part B Eng.*, vol. 270, p. 111132, Nov. 2023, doi: 10.1016/j.compositesb.2023.111132.
- [19] Y. Boon, S. Joshi, S. Bhudolia, and G. Gohel, "Recent Advances on the Design Automation for Performance-Optimized Fiber Reinforced Polymer Composite Components," *Compos. Sci.*, vol. 4, p. 60, May 2020, doi: 10.3390/jcs4020061.
- [20] A. Mohammed et al., "Modeling the Impact of Liquid Polymers on Concrete Stability in Terms of a Slump and Compressive Strength," *Appl. Sci.*, vol. 13, p. 1208, Jan. 2023, doi: 10.3390/app13021208.
- [21] E. Temizhan, H. Mirtagioglu, and M. Mendes, "Which Correlation Coefficient Should Be Used for Investigating Relations between Quantitative Variables?," *Am. Sci. Res. J. Eng. Technol. Sci.*, vol. 61, p. 5524, Dec. 2021. [Online]. Available: <https://www.researchgate.net/publication/359579944>



- [22] A. Atkinson, M. Riani, and A. Corbellini, "The Box–Cox Transformation: Review and Extensions," *Stat. Sci.*, vol. 36, pp. 239–255, 2021, doi: 10.1214/20-STS778.
- [23] J. Lu, B. Nguyen, and J. Powers, "Mechanical properties of 3 hydrophilic addition silicone and polyether elastomeric impression materials," *J. Prosthet. Dent.*, vol. 467, p. 6516, Mar. 2004, doi: 10.1016/j.prosdent.2004.05.016.
- [24] N. Mallegni, T. V. Phuong, M. B. Coltelli, P. Cinelli, and A. Lazzeri, "Poly(lactic acid) (PLA) based tear resistant and biodegradable flexible films by blown film extrusion," *Materials*, vol. 11, no. 1, p. 148, Jan. 2018, doi: 10.3390/ma11010148.
- [25] L. Aliotta et al., "Tearing fracture of poly(lactic acid) (PLA)/poly(butylene succinate-co-adipate) (PBSA) cast extruded films: Effect of the PBSA content," *Eng. Fract. Mech.*, vol. 289, p. 109450, Sep. 2023, doi: 10.1016/j.engfracmech.2023.109450.
- [26] L. Gómez-Bachar, M. Vilcovsky, P. González-Seligra, and L. Famá, "Effects of PVA and yerba mate extract on extruded films of carboxymethyl cassava starch/PVA blends for antioxidant and mechanically resistant," *Int. J. Biol. Macromol.*, vol. 268, p. 131464, Apr. 2024, doi: 10.1016/j.ijbiomac.2024.131464.
- [27] S. Kim, S. Kang, Y. Kim, and M. Park, "Industrial-scale blown active packaging film with essential oils: Properties, dual-functional performance, and box packaging application of instant noodles," *Food Packag. Shelf Life*, vol. 43, p. 101276, Apr. 2024, doi: 10.1016/j.fpsl.2024.101276.
- [28] X. Zhang, S. Ajji, and M. Huneault, "Oriented structure and anisotropy properties of polymer blown films: HDPE, LLDPE and LDPE," *Polymer*, vol. 45, pp. 217–229, Oct. 2003, doi: 10.1016/j.polymer.2003.10.057.
- [29] W. Zhou, D. Zha, X. Zhang, J. Xu, B. Gou, and Y. Huang, "Ordered long-period stacking ordered phase..." [Incompleta en el texto original].
- [30] B. Zhu et al., "Enhancing the mechanical properties of polylactic acid (PLA) composite films using *Pueraria lobata* root microcrystalline cellulose," *Int. J. Biol. Macromol.*, vol. 279, p. 135579, Nov. 2024, doi: 10.1016/j.ijbiomac.2024.135579.
- [31] I. Witten, "Inducing model trees for continuous classes," 1997. [Online]. Available: <https://www.researchgate.net/publication/2737587>
- [32] S. Altarazi, M. Ammouri, and A. Hijazi, "Artificial neural network modeling to evaluate polyvinylchloride composites' properties," *Comput. Mater. Sci.*, vol. 153, pp. 1–9, Oct. 2018, doi: 10.1016/j.commatsci.2018.06.003.
- [34] K. Balkey, A. Domenic, A. Guzmán, and S. Weinman, "Ejemplos de uso de códigos y normas para los estudiantes de ingeniería mecánica y otros campos," 2021. [Online]. Available: <http://www.asme.org/about-asme>
- [35] A. Gaspar-Cunha, J. A. Covas, and J. Sikora, "Optimization of polymer processing: A review (Part II - Molding technologies)," *Materials*, vol. 15, no. 3, p. 1138, Feb. 2022, doi: 10.3390/ma15031138.



Derechos de Autor (c) 2026 Gilberto Alarcón Aguilar, Alam Josué Reyes López, Frixia Galán-Méndez



Este texto está protegido por una licencia [Creative Commons 4.0](https://creativecommons.org/licenses/by/4.0/).

Usted es libre para compartir —copiar y redistribuir el material en cualquier medio o formato — y adaptar el documento — remezclar, transformar y crear a partir del material— para cualquier propósito, incluso para fines comerciales, siempre que cumpla la condición de:

Atribución: Usted debe dar crédito a la obra original de manera adecuada, proporcionar un enlace a la licencia, e indicar si se han realizado cambios. Puede hacerlo en cualquier forma razonable, pero no de forma tal que sugiera que tiene el apoyo del licenciante o lo recibe por el uso que hace de la obra.

[Resumen de licencia](#) - [Texto completo de la licencia](#)